IEICE Electronics Express, Vol.8, No.19, 1633–1639

PAPR reduction by a single adaptive all-pass filter for OFDM systems

Eonpyo Hong, Hyunju Kim, and Dongsoo Har[a)]

Gwangju Institute of Science and Technology (GIST),
261 Cheomdan-gwagiro, Buk-gu Gwangju, 500–712, Republic of Korea
a) *hardon@gist.ac.kr*

Abstract: This letter proposes an adaptive all-pass filter (A2PF) based peak-to-average power ratio (PAPR) reduction scheme for signle input single output orthogonal frequency division multiplexing (OFDM) systems. A properly phase rotated OFDM symbol of reduced PAPR is generated by an A2PF with its filter coefficient found by the Newton-Raphson method. For the A2PF scheme, costly side information (SI) transmission is not needed unlike the selected mapping (SLM) scheme. The A2PF scheme achieves PAPR reduction performance comparable to the SLM scheme. Simulation results demonstrate that the A2PF scheme without SI leads to BER performance close to the SLM scheme with SI.

Keywords: adaptive all-pass filter, Newton-Raphson method, orthogonal frequency division multiplexing (OFDM), peak-to-average power ratio (PAPR)
Classification: Wireless communication hardware

References

[1] R. W. Bäuml, R. F. H. Fischer, and J. B. Huber, "Reducing the peak-to-average power ratio of multicarrier modulation by selected mapping," *Electron. Lett.*, vol. 32, no. 22, pp. 2056–2057, Oct. 1996.
[2] A. Ghassemi and T. A. Gulliver, "Partial selected mapping OFDM with low complexity IFFTs," *IEEE Commun. Lett.*, vol. 12, no. 1, pp. 4–6, Jan. 2008.
[3] M. Ohta, A. Iwase, and K. Yamashita, "Improvement of the error characteristics of N-continuous OFDM system by SLM," *IEICE Electron. Express*, vol. 7, no. 18, pp. 1354–1358, Sept. 2010.
[4] E. Hong and D. Har, "Peak-to-average power ratio reduction in OFDM systems using all-pass filters," *IEEE Trans. Broadcast.*, vol. 56, no. 1, pp. 114–119, March 2010.
[5] T. I. Laakso and V. Välimaki, "Energy-based effective length of the impulse response of a recursive filter," *IEEE Trans. Instrum. Meas.*, vol. 40, no. 1, pp. 7–17, Feb. 1999.
[6] S. Kang, Y. Ha, and E. Joo, "A comparative investigation on channel estimation algorithms for OFDM in mobile communications," *IEEE Trans. Broadcast.*, vol. 49, no. 2, pp. 142–148, June 2003.
[7] ETSI ETS 300 744, "Digital video broadcasting (DVB); frame structure, channel coding, and modulation for digital terrestrial television (DVB-

DOI: 10.1587/elex.8.1633
Received August 30, 2011
Accepted September 05, 2011
Published October 10, 2011

T)," *ETSI, Tech. Rep.*, Jan. 2001.
[8] G. B. Thomas, N. D. Weir, J. Hass, and F. R. Giordano, *Thomas calculus*, Pearson, 2005.
[9] H. Ryu, J. Park, and J. Park, "Threshold IBO of HPA in the predistorted OFDM communication system," *IEEE Trans. Broadcast.*, vol. 50, no. 4, pp. 425–428, Dec. 2004.
[10] COST 207 management committee, *COST 207: Digital land mobile radio communication*, Commission of the European Communities, 1989.

1 Introduction

The selected mapping (SLM) scheme [1, 2, 3] is an attractive solution for peak-to-average power ratio (PAPR) reduction in orthogonal frequency division multiplexing (OFDM) systems, because of its high PAPR reduction performance without in-band signal distortion and out-of-band radiation. However, it requires multiple inverse fast Fourier transform (IFFT) modules and costly side information (SI) transmission. In this letter, an adaptive all-pass filter (A2PF) scheme based on a single first-order A2PF is proposed. The single A2PF replaces multiple all-pass filters of fixed filter coefficients used in [4].

2 System model with proposed A2PF scheme

2.1 Signal for A2PF

With the pilot symbols of L spacing inserted into the data symbol vector $\mathbf{S}_d$, the frequency domain OFDM symbol $\mathbf{S}$ in Fig. 1 can be represented as $\mathbf{S} = [S_p(0), S_d(0), \ldots, S_d(L-2), S_p(1), S_d(L-1), \ldots, S_d(N_d-1), S_p(N_p-1)]^T \triangleq [S(0), S(1), \ldots, S(N_v-1)]^T$, where subscripts d, p, N_d, N_p stand for modulated data symbol, modulated pilot symbol, the number of data symbols, the number of pilot symbols, respectively. Note that the number of valid symbols $N_v = N_p + N_d$. The time domain symbol vector $\mathbf{s} = [s(0), s(1), \ldots, s(N-1)]^T$, where N represents the number of total symbols including null symbols, is given by an IFFT operation as $s(n) = \sum_{k=0}^{N_v-1} S(k) e^{j2\pi kn/N} / \sqrt{N_v}$. The PAPR of $\mathbf{s}$ is given by $\max_{0 \le n \le N-1} |s(n)|^2 / E[|s(n)|^2]$.

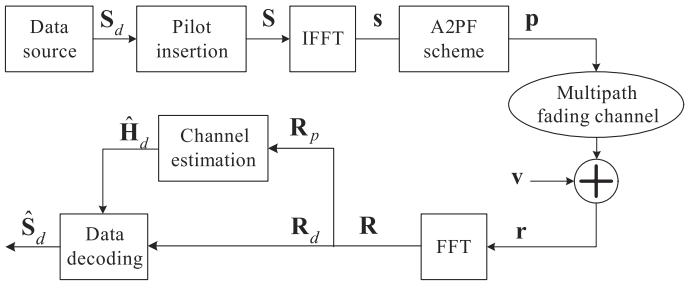

Fig. 1. Block diagram (without insertion and removal of guard interval) of OFDM systems with the A2PF scheme.

DOI: 10.1587/elex.8.1633
Received August 30, 2011
Accepted September 05, 2011
Published October 10, 2011

2.2 Transmitted signal from A2PF

The frequency response of the first-order A2PF is given by $F(e^{j2\pi k/N}) = (e^{-j2\pi k/N}+c)/(1+c^*e^{-j2\pi k/N})$, where c is the filter coefficient. The phase rotated time domain symbol vector $\mathbf{p}$ is obtained by a circular convolution of the input $\mathbf{s}$ with the impulse response vector $\mathbf{f} = [f(0), f(1), \ldots, f(N_e-1)]^T$ of the A2PF, where N_e is the effective length of the impulse response [5]. To perform a circular convolution by a linear convolution of the A2PF, cyclic prefix (CP) with its length N_c greater than N_e is placed at the beginning of $\mathbf{s}$ [4]. The $\mathbf{s}$ with CP is given as $\tilde{\mathbf{s}} = [s(N-N_c), \ldots, s(N-1), s(0), \ldots, s(N-1)]^T = [\tilde{s}(0), \tilde{s}(1), \ldots, \tilde{s}(N+N_c-1)]^T$. With $\tilde{\mathbf{s}}$ as the input of the A2PF, the output $\tilde{\mathbf{p}}_c = [\tilde{p}_c(0), \ldots, \tilde{p}_c(n), \ldots, \tilde{p}_c(N+N_c-1)]^T$ is obtained by

$$\tilde{p}_c(n) = \tilde{s}(n-1)+c\tilde{s}(n)-c^*\tilde{p}_c(n-1) \tag{1}$$

where $\tilde{s}(-1)$ and $\tilde{p}_c(-1)$ are set to zero because their indices correspond outside to a time domain OFDM symbol. By removing the output of CP, the time domain symbol vector $\mathbf{p} = [\tilde{p}_c(N_c), \tilde{p}_c(N_c+1), \ldots, \tilde{p}_c(N+N_c-1)]^T$ is transmitted with a guard interval filled with yet another CP to avoid inter-symbol interference.

2.3 Received signal at receiver

The frequency domain symbol vector $\mathbf{R} = [R(0), R(1), \ldots, R(N_v-1)]^T$ obtained from FFT module in Fig. 1 is given as

$$R(k) = H(k)F(e^{j2\pi k/N})S(k) + V(k) \tag{2}$$

where $H(k)$ is the k-th sub-channel response and $V(k)$ is an i.i.d. complex additive white Gaussian noise (AWGN). The pilot symbol vector $\mathbf{R}_p = [R_p(0), R_p(1), \ldots, R_p(N_p-1)]^T$ embedded in $\mathbf{R}$ can be represented as

$$R_p(l) = H_p(l)F_p(l)S_p(l) + V_p(l) \tag{3}$$

where $H_p(l)$, $F_p(l)$, $V_p(l)$ of the l-th pilot sub-channel are the channel response, the phase rotation by the A2PF, the complex AWGN, respectively. In (3), the estimate by the least square estimation of the l-th pilot sub-channel response is given as $\hat{H}_p(l) = R_p(l)/S_p(l)$ [4]. The estimate of data sub-channel response $\hat{H}_d(k)$, where $k = l(L-1), l(L-1)+1, \ldots, l(L-1)+L-2$, is acquired by the cubic spline interpolation of the adjacent pilot symbols [6]. Due to smooth phase shift of $F(e^{j2\pi k/N})$, data sub-channel estimation by the interpolation can be successfully used. Data symbol $\hat{S}_d(k)$ is recovered by a decision metric as following

$$D = \min_{\hat{S}_d(k)\in Q} |R_d(k) - \hat{H}_d(k)\hat{S}_d(k)|^2 \tag{4}$$

where $R_d(k)$ is the received data symbol and Q is the normalized constellation [7] given for $S_d(k)$.

DOI: 10.1587/elex.8.1633
Received August 30, 2011
Accepted September 05, 2011
Published October 10, 2011

3 Newton-Raphson method

The filter coefficient c reducing the PAPR of $\mathbf{p}$ is iteratively found by the Newton-Raphson (NR) method [8]. The cost function is defined as

$$\phi(c_i) = |\tilde{p}_{c_i}(n_i)|^2 - \eta \tag{5}$$

where c_i is c at the i-th iteration and $n_i = \arg\max_{n\in\{N_c\le n\le N+N_c-1\}} |\tilde{p}_{c_i}(n)|^2$ is the index of peak power at the i-th iteration and η is the scalable target PAPR. The n_i is subject to change during iterations and $\tilde{p}_{c_i}(n_i)$ is varied according to c_i. The $|\tilde{p}_{c_i}(n_i)|^2$ is the PAPR at the i-th iteration with the normalized signal power $E[|\tilde{p}_{c_i}(n)|^2] = E[|\tilde{s}(n)|^2] = 1$. The coefficient c_i satisfying $\phi(c_i)\le 0$ is sought, since c_i satisfying such condition leads to PAPR less than or equal to η. The c_{i+1} for the given $\tilde{\mathbf{s}}$ is updated from c_i as following

$$c_{i+1} = c_i - (\phi(c_i)/\phi'(c_i)) \tag{6}$$

The $\phi'(c_i)$ is obtained by

$$\phi'(c_i) = \frac{\partial(|\tilde{p}_{c_i}(n_i)|^2 - \eta)}{\partial c_i} = \tilde{p}^*_{c_i}(n_i)d_i(n_i) + \tilde{p}_{c_i}(n_i)g_i(n_i) \tag{7}$$

where $d_i(n_i) = \partial(\tilde{p}_{c_i}(n_i))/\partial c_i$ and $g_i(n_i) = \partial(\tilde{p}^*_{c_i}(n_i))/\partial c_i$. The functional dependency of continuous c_i on discrete n_i is ignored, so an ad hoc solution is produced in (7). The recursive equations for $d_i(n_i)$ and $g_i(n_i)$ can be obtained as

$$d_i(n_i) = \tilde{s}(n_i) - c_i^* d_i(n_i - 1) \tag{8}$$

$$g_i(n_i) = -\tilde{p}^*_{c_i}(n_i - 1) - c_i g_i(n_i - 1) \tag{9}$$

with the boundary values $d_i(-1) = g_i(-1) = \tilde{p}^*_{c_i}(-1) = 0$, due to $\tilde{s}(-1) = 0$ and $\tilde{p}_{c_i}(-1) = 0$. With c_{i+1}, $\tilde{p}_{c_{i+1}}(n_{i+1})$ is updated and new cost is evaluated by (5). The c_0 is set to zero and then the PAPR is checked whether it satisfies the target PAPR. If so, (6) is skipped and next OFDM symbol is considered.

The magnitude of the coefficient is confined to $|c_i| < \lambda$, where $0 < \lambda < 1$, to ensure that the pole of the A2PF is within a unit circle for stability. If the magnitude of c_{i+1} is larger than λ, c_{i+1} is randomly acquired by $\mathbf{A}e^{j\mathbf{\Phi}}$, where $\mathbf{A}$ and $\mathbf{\Phi}$ are uniformly distributed over 0 to λ and over 0 to 2π, respectively. With such $\mathbf{A}$ and $\mathbf{\Phi}$, further iterations are performed.

4 Computational complexity and simulation results

Total number of sub-carriers N is chosen as 64, 512, 2048. Considering the working range 10^{-4} to 10^{-2} of complementary cumulative distribution function (CCDF) of PAPR falling into approximately 8–9 dB range of PAPR values, the number of independent phase sequences $U = 4, 6, 8$ is considered for the SLM scheme. The target PAPR $\eta = 7.5$, 8.5, and 9 dB are selected for the A2PF scheme. The λ is set to 0.9 and $N_c = 64$ which is much larger than the maximum $N_e \approx 3$ when $|c_i| = 0.9$.

Computational complexity of the A2PF scheme is compared with those of the SLM scheme [1] and the partial SLM (P-SLM) scheme [2]. Computational

DOI: 10.1587/elex.8.1633
Received August 30, 2011
Accepted September 05, 2011
Published October 10, 2011

complexities of the SLM scheme and the P-SLM scheme are specified in [2]. For the P-SLM scheme, $\sum_{b=1}^{\zeta-1}2^{b-1}(N/2^b-1)+(U/2)\sum_{b=\zeta}^{B}2^{b-1}(N/2^b-1)$ complex multiplications and $N[\zeta+U(B-\zeta)/2]$ complex additions are required for $B=\log_2 N$ and optimal $\zeta = B-2$. The SLM scheme and the P-SLM scheme commonly need additional UN complex multiplications to get the peak power of U phase rotated time domain symbols for $0\leq n\leq N-1$.

With a single IFFT module of the A2PF scheme, $(N/2)\log_2 N$ complex multiplications and $N\log_2 N$ complex additions are necessary. From (8) and (9), the most pessimistic computational complexity of $d_i(N+N_c-1)$ and $g_i(N+N_c-1)$ per iteration is $2(N_c+N)$ complex multiplications and $2(N_c+N)$ complex additions with $n_i=N+N_c-1$. A few complex multiplications and complex additions in (6) and (7) are neglected. For filtering operation in (1), $2(N_c+N)$ complex multiplications and $2(N_c+N)$ complex additions are required and N complex multiplications to get $|\tilde{p}_{c_i}(n_i)|^2$ are additionally needed. As a whole, considering the average number of iterations i_{ave}, the total numbers of complex multiplications and complex additions are given as $(N/2)\log_2 N+4i_{ave}(N_c+N)+N(i_{ave}+1)$ and $N\log_2 N+4i_{ave}(N_c+N)$, respectively. Finding $|\tilde{p}_{c_i}(n_i)|^2$ over N samples is not considered for computational complexity evaluation. Table I shows the computational complexity reduction ratio (CCRR) of the P-SLM scheme and the A2PF scheme with respect to the SLM scheme. The A2PF scheme is comparable to the P-SLM scheme and computational gain of the A2PF scheme over the SLM scheme is increased with larger N and/or U.

Fig. 2 (a) shows the CCDF of PAPR. The CCDF value of the A2PF scheme drops sharply at the target PAPR, because the iteration to find proper filter coefficient is continued until the target PAPR is achieved. Over the working range of CCDF 10^{-4} to 10^{-2}, the A2PF scheme seems competitive to the SLM scheme. Fig. 2 (b) shows the probability that the PAPR of an OFDM symbol exceeds the target PAPR η as the number of iterations increases. As observed in the figure, few iterations are needed for most OFDM symbols. The target PAPR is satisfied within 50 iterations at CCDF level

Table I. CCRR of the P-SLM scheme with SI and the A2PF scheme without SI with respect to the SLM scheme.

Type of complex operations	Parameters	P-SLM scheme with SI	A2PF scheme without SI
$\times$s	N=64, U=4, η=7.5 dB, i_{ave}=0.28	58.5 %	62.8 %
	N=512, U=6, η=8.5 dB, i_{ave}=0.56	67.4 %	74.4 %
	N=2048, U=8, η=9 dB, i_{ave}=1.11	72.4 %	76.7 %
+s	N=64, U=4, η=7.5 dB, i_{ave}=0.28	66.7 %	68.0 %
	N=512, U=6, η=8.5 dB, i_{ave}=0.56	75.9 %	78.9 %
	N=2048, U=8, η=9 dB, i_{ave}=1.11	80.7 %	82.4 %

† $\times$ and + represent complex multiplications and complex additions .
N=total number of symbols , U=number of phase symbol vectors for SLM scheme ,
η=target PAPR for A2PF scheme, i_{ave}=average number of iterations for A2PF scheme

$$\text{CCRR}=\left(1-\frac{\text{complexity of the given scheme}}{\text{complexity of the SLM scheme}}\right)\times 100\ [\%]$$

DOI: 10.1587/elex.8.1633
Received August 30, 2011
Accepted September 05, 2011
Published October 10, 2011

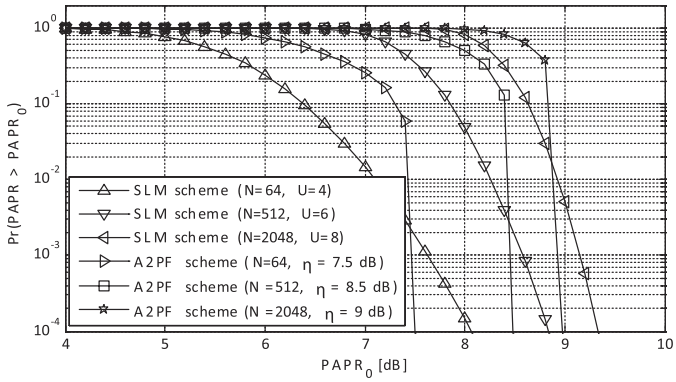

(a) CCDF of PAPR for the SLM scheme and the A2PF scheme.

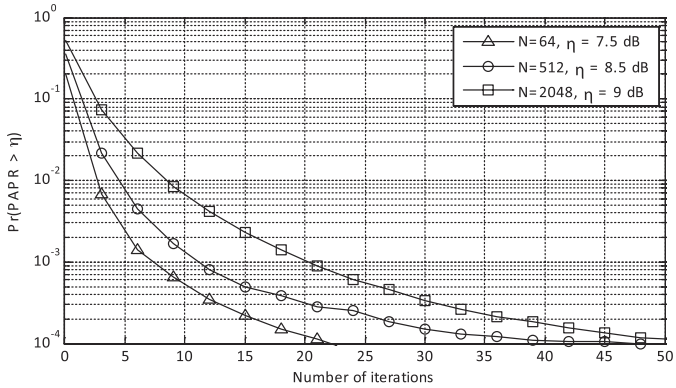

(b) Probability that PAPR of an OFDM symbol vector exceeds the target PAPR η with the A2PF scheme according to the number of iterations.

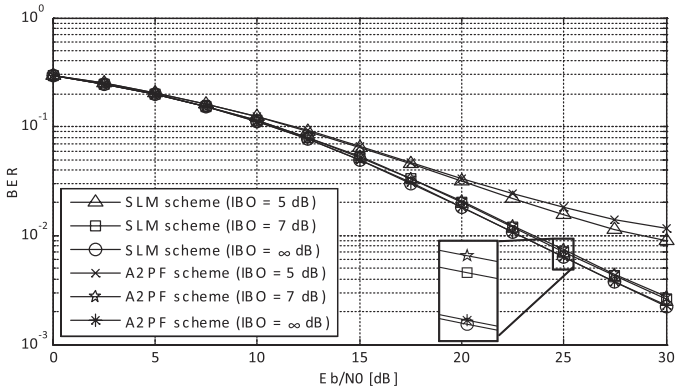

(c) BER performance of the SLM scheme with $U = 8$ and the A2PF scheme with $\eta = 9$ dB.

Fig. 2. PAPR reduction performance and BER performance of the A2PF scheme.

10^{-4}. Generally, lower η value with fixed N leads to increased i_{ave} and larger N for fixed η value leads to increased i_{ave}.

Fig. 2 (c) shows the BER performance of the A2PF scheme. Simulations were performed complying with the digital video broadcasting for terrestrial (DVB-T) standard [7]: $N = 2048$, $N_v = 1705$, OFDM symbol duration $= 224\,\mu$s, The scattered pilot symbol spacing $L = 12$. Pilot symbols are modulated by binary PSK and data symbols are modulated by 64-QAM. The solid state power amplifier model with nonlinear parameter = 3 and input

DOI: 10.1587/elex.8.1633
Received August 30, 2011
Accepted September 05, 2011
Published October 10, 2011

back-off (IBO) = 5 dB, 7 dB, ∞ dB is considered for the nonlinear power amplifier (NPA) [9]. The ∞ dB implies no NPA at transmitter. The urban (TU-6) channel specified in [10] is used for simulations. The A2PF scheme without SI achieves almost the same performance as that of the SLM scheme with SI. A little degradation of the A2PF scheme over the SLM scheme with IBO=5 dB is due to erroneous channel estimation with the phase shifted data symbols.

5 Conclusions

The proposed A2PF scheme without SI leads to PAPR reduction performance comparable to the SLM scheme with SI for the considered system parameters. Simple channel estimation based on pilot symbols enables SI-free data recovery, leading to the BER performance close to the SLM scheme with SI. Computational gain of the A2PF scheme over the SLM scheme is remarkable with the system parameters considered.

Acknowledgments

This work was supported by Center for Distributed Sensor Network at GIST.

DOI: 10.1587/elex.8.1633
Received August 30, 2011
Accepted September 05, 2011
Published October 10, 2011